Green's function solution to subsurface light transport for BRDF computation

Charly Collin* University of Central Florida
Ke Chen† University of Central Florida
Ajit Hakke-Patil‡ University of Central Florida
Sumanta Pattanaik§ University of Central Florida
Kadi Bouatouch ¶ IRISA, Université de Rennes 1

Abstract

This paper presents an accurate method to compute the bidirectional reflectance distribution function (BRDF) due to subsurface scattering inside the material of the objects. This computation requires iterating over the different lighting directions, and solving the integro-differential equation of light transport (scattering and absorption). Solving the light transport equation is expensive, and solving it independently for different directions adds even further to the expense. However most of the computations are very similar between directions. We make use of Green's function of the transport problem to have a better separation between computations that are independent of incident directions from those that are dependent. This allows us to avoid as much repetition in the computations as possible, thus gives us a faster BRDF computation method without any loss of accuracy. We validate our method against a standard light transport solver and use it to compute BRDF for a variety of materials.

CR Categories: I.3.0 [Computer Graphics]: General—; I.4.1 [Image Processing and Computer Vision]: Digitalization and Capture—Reflectance

Keywords: BRDF, subsurface scattering, discrete-ordinates method, light transport, layered materials

1 Introduction

Accurately modeling the bidirectional reflectance distribution function (BRDF) [Nicodemus 1967] of materials is an important step in realistic rendering. BRDF for most real world materials may be modeled as a combination of two components: specular, the component resulting from surface only interaction of light, and diffuse, the component resulting from subsurface interaction of light [Dorsey et al. 2008][Hanrahan and Krueger 1993]. The discussions in this paper is limited to the diffuse component of BRDF. Lambertian model is a convenient idealization of the diffuse BRDF, where BRDF is assumed to be a constant, independent of incident and outgoing direction. However, diffuse BRDF of most materials have significant directional dependence, and computing them accurately requires accurate solution of subsurface interaction of light.

Light interaction inside the volume of the material can be modeled by an integro-differential equation known as the radiative transfer equation or the RTE. Its solution is expensive. Solving the RTE for BRDF computation requires one to solve the RTE for a large number of incident directions, thus making the computation all the more expensive. Of the various methods, discrete ordinate based method is one of the widely used methods for accurate computations of the RTE solutions.

In this paper, we focus on efficiently computing the RTE solution using a discrete ordinate based method (DOM). We propose a Green's function based method to accelerate this solution method for BRDF computation. We show that while being convenient to compute, the Green's function reduces the impact of increasing the number of lighting directions towards the overall computation time. We demonstrate the usefulness of the method in computing diffuse BRDF for many real world materials. We validate the computation results with solutions from a standard RTE solver available in Optics literature. We compare the efficiency of our Green's function based solution for BRDF with commonly used DOM solution approach.

The following is a brief outline of the paper. In the next section we review existing work. In section 3 we provide a background to radiative transport equation and Green's function. In section 4 we detail our Green's function based DOM computation method. We describe the results of our implementation in section 5.

2 Related work

Like clouds and atmosphere, most materials we come across in the real world may be considered to be composed of particles (or pigments) that scatter and absorb light. The type, density and orientation define the property of the material. While light can easily go through most clouds, most of the interaction in a so called opaque material happens in a microscopic layer below the surface. This interaction is termed subsurface interaction. A part of the scattered light from the subsurface interaction comes out of the surface, and it is this light that makes up the diffuse component of BRDF. Many efforts have been made to account for this component in BRDF formulations, some of which we describe here.

In order to remain efficient, several methods only approximate subsurface scattering. Kubelka-Munk [Kubelka 1948] method is one such method that provides a simple formulation for the reflectance from materials composed of one or more pigment layers. This method is efficient, but uses a two streams approximation for the radiance field. That means it approximates all the directions of the radiance field by one upward and one downward direction, which is not enough to take into account directionality in diffuse reflectance computation. Originally used in medical physics domain, the diffusion approximation theory has found use in computing subsur-

*e-mail: charly.collin@bobbyblues.com
†e-mail:chenke@knights.ucf.edu
‡e-mail:ajitpatil@knights.ucf.edu
§e-mail:sumant@cs.ucf.edu
¶e-mail:kadi@irisa.fr

face scattering for BRDF [Stam 1995]. Jensen et al [2001] through the dipole model, proposed a simple solution based on diffusion approximation. As in Kubelka-Munk model the diffusion approximation computes a diffuse BRDF that is independent of outgoing directions.

Several accurate methods for subsurface scattering based BRDF computation have also been proposed in the literature. Dorsey et al. [1999] used a photon mapping based computation of subsurface scattering, Hanrahan and Kruger [1993] and Pharr and Hanrahan [2000] used Monte Carlo path tracing based methods for solving the RTE for BRDF computation. While these methods can correctly simulate all scattering events, noise free accurate BRDF computation using these Monte Carlo based methods can be very expensive computationally, especially for materials that are highly scattering. In the case of layered materials, the adding doubling method [de Haan et al. 1987] gives accurate results, but has been noted for its high computational cost. Finally, discrete ordinates methods [Chandrasekhar 1960] have also been widely used for accurately solving the RTE in layered atmosphere, but have not found wide use in BRDF computation because of the cost involved.

In an attempt to improve the efficiency of the discrete ordinate based method for BRDF computation, we propose a Green's function based approach to solving one of the main steps of the method.

3 Background

Our goal in this paper is to compute the BRDF due to subsurface scattering. BRDF is defined as the radiance reflected from a surface point as a function of the irradiance incident from any direction in the incoming hemisphere [Nicodemus 1967], and can be expressed as:

$$f_r(\mu_{inc},\phi_{inc},\mu,\phi) = \frac{I(0,\mu,\phi)}{E_{inc}(\mu_{inc},\phi_{inc})} \tag{1}$$

where μ is the cosine of the zenith angle as measured from the normal to the surface of the material and ϕ is the azimuth angle, (μ_{inc},ϕ_{inc}) and (μ,ϕ) are the incoming and reflected directions respectively, $I(\tau,\mu,\phi)$ is the radiance at an optical thickness of τ (measured from the surface of the material) along direction (μ,ϕ) and E_{inc} is the irradiance along the incoming direction.

We will assume that the material is a plane parallel medium, i.e. the scattering and absorption property of the material varies only along the depth (the direction perpendicular to the plane). So the material property is defined by phase function p and single scattering albedo ω that are functions of optical thickness τ. We assume that the particles in the medium that interact with the light are spherical or randomly oriented, thus making p a function of only the scattering angle θ formed by the incoming and scattered direction. The resulting BRDF f_r becomes a function of only 3 parameters: $f(\mu_{inc},\mu,\phi-\phi_{inc})$. Without any loss of generality we will set ϕ_{inc} to zero and represent BRDF as $f(\mu_{inc},\mu,\phi)$.

For computing BRDF we need the radiance field at the surface of the material i.e. at $\tau = 0$, resulting from the subsurface interaction of the incident light from any direction $(\mu_{inc},0)$. The radiance field due to subsurface light transport in plane parallel media may be modeled as the solution to the radiative transfer equation (RTE)[Chandrasekhar 1960]:

$$\mu\frac{\partial}{\partial\tau}I(\tau,\mu,\phi)+I(\tau,\mu,\phi)-J(\tau,\mu,\phi) = Q(\tau,\mu,\phi) \tag{2}$$

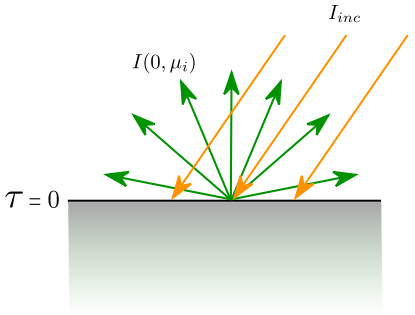

Figure 1: Computing the BRDF requires computing the radiance field (in green) at the top of the material for each incoming direction of a parallel light source (in yellow).

The J term in the equation is defined as:

$$J(\tau,\mu,\phi) = \frac{\omega(\tau)}{4\pi}\int_{-1}^{1}\int_{0}^{2\pi} p(\tau,\theta')I(\tau,\mu',\phi')d\phi' d\mu' \tag{3}$$

with $p(\tau,\theta')$ the phase function at optical thickness τ, θ' the angle between the incoming direction (μ',ϕ') and the outgoing direction (μ,ϕ). The Q function accounts for radiance due to the incident I_{inc} from direction (μ_{inc},ϕ_{inc}), and is expressed as:

$$Q(\tau,\mu,\phi) = \frac{\omega(\tau)I_{inc}(\mu_{inc})}{4\pi}p(\tau,\theta)e^{-\tau/\mu_{inc}} \tag{4}$$

where θ is the angle between the incident direction $(\mu_{inc},0)$ and the outgoing direction (μ,ϕ).

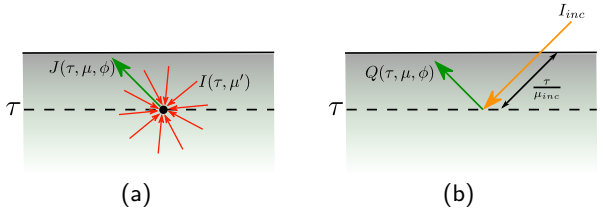

Figure 2: The J term (a) corresponds to scattered radiance at optical depth τ along direction (μ,ϕ) due to the radiance incoming from all directions. The inhomogeneous term Q (b) accounts for the radiance due to the scattering attenuated incident radiance.

Unlike most of the DOM based method used in Computer Graphics literature that use space and direction discretization followed by iterative solution, our method is based on another commonly used DOM approach used in Optical literature that involves Fourier expansion, homogeneous and particular solution computation. This method of solving the RTE starts with reducing the dimensionality of the radiance functions involved, which is done by expanding the radiance in the truncated Fourier series as [Sobolev 1975]:

$$I(\tau,\mu,\phi) = \frac{1}{2}I^0(\tau,\mu)+\sum_{m=1}^{L} I^m(\tau,\mu)\cos(m\phi), \tag{5}$$

Independent expressions for $I^m(\tau,\mu)$'s are developed by first expanding $p(\tau,\theta')$ in truncated Legendre polynomial series as:

$$p(\tau,\theta') = \sum_{m=0}^{L} g_m(\tau)P_m(\cos\theta')$$

then rewriting it using the relation

$$\cos\theta' = \mu\mu' + \sqrt{(1-\mu^2)(1-\mu'^2)}\cos(\phi-\phi')$$

as

$$p(\tau,\theta') = p^0(\tau,\mu,\mu') + 2\sum_{m=1}^{L} p^m(\tau,\mu,\mu')\cos\left(m(\phi-\phi')\right) \quad (6)$$

$$\text{where} \quad p^m(\tau,\mu,\mu') = \sum_{l=m}^{L} g_l(\tau)P_l^m(\mu)P_l^m(\mu'),$$

and P_l^m's are the normalized associated Legendre polynomials.

Using these expansions, the RTE equation for $I^m(\tau,\mu)$ can be written as:

$$\mu\frac{\partial I^m(\tau,\mu)}{\partial\tau} + I^m(\tau,\mu) - \frac{\omega(\tau)}{2}\int_{-1}^{1} p^m(\tau,\mu,\mu')I^m(\tau,\mu')d\mu' = Q^m(\tau,\mu) \quad (7)$$

or in a compact operator notation as:

$$\mathscr{L}[I^m(\tau,\mu)] = Q^m(\tau,\mu) \quad (8)$$

where

$$Q^m(\tau,\mu) = \frac{\omega}{4}p^m(\tau,\mu,\mu_{inc})I_{inc}(\mu_{inc})e^{-\tau/\mu_{inc}} \quad (9)$$

and $\mathscr{L}$ an integro-differential operator as expanded in equation 7.

In classic differential equations literature, equations similar to (8) are called inhomogeneous equations, and Q^m's on the right hand side are called the inhomogeneous terms. A standard way to computing the solution to inhomogeneous equations is: find solution I_h^m to the homogeneous form of the equation such that,

$$\mathscr{L}[I_h^m(\tau,\mu)] = 0 \quad (10)$$

and then find a particular solution I_p^m that satisfies the original equation, i.e.

$$\mathscr{L}[I_p^m(\tau,\mu)] = Q^m(\tau,\mu) \quad (11)$$

and compose the final solution as a combination of the two, i.e. $I^m = I_h^m + I_p^m$.

Given that our goal is to compute BRDF, we must compute the radiance field separately for a large number of incident directions. Change in incident direction changes the inhomogeneous term in equation 9. So the classical approach of solving equation 8 would require us to compute the particular solution separately for each incident direction. This approach of particular solution computation for our problem (see Appendix) requires solving a linear system of size N, where N is the number of quadrature nodes used to compute the integration term in equation 7. For BRDF computation this process must be repeated for every incident direction and when computed for a large number of incident directions the overall computation can become expensive. Providing a relatively efficient solution is the main motivation behind the work presented in this paper, and towards this goal we propose a Green's function based efficient particular solution approach. In the remaining part of this section we provide a quick review of the Green's function and a general method of finding particular solution using Green's function. In the following section we detail the solution specific to our equations.

The Green's function for the type of equations shown in (11) is defined as the solution to the following equation:

$$\mathscr{L}[G^m(\tau,\mu:t,\mu'')] = \delta(t-\tau)\delta(\mu''-\mu) \quad (12)$$

This equation is also an inhomogeneous equation, but has a product of delta functions as the inhomogeneous term. Because of these delta functions we can write the following relation:

$$\int_0^{\tau_0}\int_{-1}^{1}\mathscr{L}[G^m(\tau,\mu:t,\mu'')]Q^m(t,\mu'')dtd\mu'' = Q^m(\tau,\mu) \quad (13)$$

where τ_0 is the thickness of the material layer. This relationship is valid for any function of (t,μ''). We wrote the equation with Q^m function deliberately so that the right hand side of this equation matches with the right hand side of equation 11. This in turn implies that

$$\begin{aligned}\mathscr{L}[I_p^m(\tau,\mu)] &= \int_0^{\tau_0}\int_{-1}^{1}\mathscr{L}[G^m(\tau,\mu:t,\mu'')]Q^m(t,\mu'')dtd\mu'' \\ &= \mathscr{L}\left[\int_0^{\tau_0}\int_{-1}^{1}G^m(\tau,\mu:t,\mu'')Q^m(t,\mu'')dtd\mu''\right]\end{aligned}$$

from which we get the relation:

$$I_p^m(\tau,\mu) = \int_0^{\tau_0}\int_{-1}^{1}G^m(\tau,\mu:t,\mu'')Q^m(t,\mu'')dtd\mu'' \quad (14)$$

That means we can apply a quadrature technique to the right hand side of equation 14 to compute the particular solution $I_p^m(\tau,\mu)$.

Another advantage of having the delta function in the definition of Green's function is that for any $\tau \neq t$, equation 12 is a homogeneous equation, i.e.

$$\mathscr{L}[G^m(\tau,\mu:t,\mu'')] = 0$$

and if we have already computed the solution of equation 10 then the solution to the homogeneous equation shown here can be assembled with very little extra effort.

Furthermore, integrating equation 12 with respect to τ in the interval $t-\varepsilon$ and $t+\varepsilon$ for $\varepsilon \to 0$, i.e.

$$\int_{t-\varepsilon}^{t+\varepsilon}\mathscr{L}[G^m(\tau,\mu:t,\mu'')]dt = \int_{t-\varepsilon}^{t+\varepsilon}\delta(t-\tau)\delta(\mu''-\mu)dt$$

we get the relation

$$\mu[G^m(t+\varepsilon,\mu:t,\mu'') - G^m(t-\varepsilon,\mu:t,\mu'')] = \delta(\mu''-\mu) \quad (15)$$

Such a relation is termed as *jump condition* in differential equation literature. This relation along with the solution to the homogeneous solution are used to derive $G^m(\tau,\mu:t,\mu'')$, the full solution to (12), which in turn is used to compute $I_p^m(\tau,\mu)$ via equation equation 14. Note that Green's function G^m is independent of incident radiance I_{inc} and hence can be computed once, and be used to get I_p^m's for any number of incident directions. We exploit this property to derive an efficient solution to the radiance field in the next section, and use it to compute BRDF.

4 Green's Function Based Algorithm For BRDF Computation

Computation of BRDF due to subsurface interaction of incident light requires the computation of surface radiance field as a function of incident radiance from any direction in the incident hemisphere. We use a modified DOM method for solving the RTE for computation of this radiance field. We provided a brief outline of the RTE solution method in section 3: we developed the expression for the subsurface radiance field in equation 2, its Fourier expansion

in equation 5, the equation of the individual terms of expansion in equation 7, and showed that the solutions of these later terms can be constructed from their homogeneous and particular solutions. We also showed that Green's function based particular solution computation method can be efficient from the point of view of BRDF computation. In this section we elaborate on a discrete ordinate based method for computation of the homogeneous solution and a Green's function based method for computing particular solution. The methods assume that the plane parallel medium of the material is composed of multiple homogeneous layers, that means the phase function p and the surface albedo ω in each layer are independent of the layer thickness. For simplicity of explanation, we first describe solution methods for materials composed of a single homogeneous layer. We then extend the methods to account for multiple layers.

Equation 7 for a single homogeneous layer of thickness τ_0 can be rewritten as:

$$\mu \frac{\partial I^m(\tau,\mu)}{\partial \tau} + I^m(\tau,\mu) - \frac{\omega}{2}\int_{-1}^{1} p^m(\mu,\mu')I^m(\tau,\mu')d\mu' = Q^m(\tau,\mu)$$

Applying Gaussian quadrature scheme to the integral term in the equation gives us a system of N equations

$$\mu_i \frac{\partial I^m(\tau,\mu_i)}{\partial \tau} + I^m(\tau,\mu_i) - \frac{\omega}{2}\sum_{j=1}^{N} \alpha_j p^m(\mu_i,\mu_j)I^m(\tau,\mu_j) = Q^m(\tau,\mu_i) \quad (16)$$

where μ_i's and α_i's are the Gaussian quadrature angles and weights respectively.

4.1 Computing homogeneous solution I_h^m

The first step in computing $I^m(\tau,\mu_i)$, the solutions of equation 16, is to compute a homogeneous solution I_h^m that satisfies:

$$\mu_i \frac{\partial I_h^m(\tau,\mu_i)}{\partial \tau} + I_h^m(\tau,\mu_i) - \frac{\omega}{2}\sum_{j=1}^{N} \alpha_j p^m(\mu_i,\mu_j)I_h^m(\tau,\mu_j) = 0 \quad (17)$$

Following the standard practice in differential equation literature we seek exponential solutions to these equations as:

$$I_h^m(\tau,\mu_i) = \Phi^m(\mu_i)e^{-\tau/\nu} \quad (18)$$

where $\Phi^m(\mu)$ is an unknown function independent of τ, and ν an unknown coefficient. We seek the values of ν and Φ^m estimated at each discrete angle by solving the linear system (20), which results from using the relations in (18) and (19) in equation 17.

$$\frac{\partial I_h^m(\tau,\mu_i)}{\partial \tau} = -\frac{1}{\nu}\Phi^m(\mu_i)e^{-\tau/\nu} \quad (19)$$

$$-\frac{\mu_i}{\nu}\Phi^m(\mu_i) + \Phi^m(\mu_i) - \frac{\omega}{2}\sum_{j=1}^{N} \alpha_j p^m(\mu_i,\mu_j)\Phi^m(\mu_j) = 0 \quad (20)$$

The linear system shown in (20), when written in a matrix form, gives us an eigenproblem:

$$\mathscr{M}\begin{bmatrix}\Phi^m(\mu_1)\\ \Phi^m(\mu_2)\\ \vdots \\ \Phi^m(\mu_N)\end{bmatrix} = \frac{1}{\nu}\begin{bmatrix}\Phi^m(\mu_1)\\ \Phi^m(\mu_2)\\ \vdots \\ \Phi^m(\mu_N)\end{bmatrix} \quad (21)$$

where

$$\mathscr{M}_{ij} = \frac{1}{\mu_i}\left(\delta_{ij} - \frac{\omega}{2}\alpha_j p^m(\mu_i,\mu_j)\right) \quad (22)$$

δ_{ij} being the Kronecker delta function.

The solution of this eigenproblem gives us a set of N eigenvectors Φ_i^m and eigenvalues ν_i. So we express our solution to equation 17 as a linear combination of the eigenvectors:

$$I_h^m(\tau,\mu_i) = \sum_{k=1}^{N} L_k^m \Phi_k^m(\mu_i)e^{-\tau/\nu_k}. \quad (23)$$

where L_k^m's are the scalar factors that must be determined.

Thus the computation of the homogeneous solution for every m requires eigensolution of a matrix of size $N \times N$. In practice using the symmetry of the quadrature angles allows us to reduce the problem to the eigensolution of a matrix of size $\frac{N}{2} \times \frac{N}{2}$. We chose here not to differentiate positive from negative angles to keep notations clear. In our actual implementation we keep them separate to simplify the matrix set up and eigensolution computation.

4.2 Computing particular solution I_p^m using Green's function

Having described a method to compute the homogeneous solution, we now proceed to elaborate the Green's function based method for computing the particular solution. We rewrite the Green's function equation from section 3 for the single layer material as:

$$\mu_i \frac{\partial G^m(\tau,\mu_i:t,\mu_\gamma)}{\partial \tau} + G^m(\tau,\mu_i:t,\mu_\gamma) - \frac{\omega}{2}\sum_{j=1}^{N} \alpha_j p^m(\mu_i,\mu_j)G^m(\tau,\mu_j:t,\mu_\gamma) = \delta(\tau-t)\delta_{i,\gamma} \quad (24)$$

and the particular solution to equation 16 as:

$$I_p^m(\tau,\mu_i) = \sum_{\gamma=1}^{N}\int_0^{\tau_0} G^m(\tau,\mu_i:t,\mu_\gamma)Q^m(t,\mu_\gamma)dt \quad (25)$$

For any $\tau \neq t$, (24) is a homogeneous equation. So, like in (23), we construct its solution from the eigensolution of equation 21. Because of the discontinuities at t we construct the solution separately for $\tau < t$ and for $\tau > t$.

$$G^m(\tau > t,\mu_i:t,\mu_\gamma) = \sum_{k=1}^{J} A_{k,\gamma}^m \Phi_k^m(\mu_i)e^{-(\tau-t)/\nu_k} \quad (26)$$

$$G^m(\tau < t,\mu_i:t,\mu_\gamma) = -\sum_{k=J+1}^{N} B_{k,\gamma}^m \Phi_k^m(\mu_i)e^{(t-\tau)/\nu_k} \quad (27)$$

Substituting those formulations for $\tau = x$ in the *jump condition* (15) yields:

$$\mu_i \sum_{k=1}^{J} A_{k,\gamma}^m \Phi_k^m(\mu_i) + \mu_i \sum_{k=J+1}^{N} B_{k,\gamma}^m \Phi_k^m(\mu_i) = \delta_{i\gamma} \quad (28)$$

Note the difference in the exponential terms here from that in (23). This takes into account the fact that the inhomogeneous term here is introduced from $\tau = t$, whereas homogeneous term of the RTE equation is introduced from $\tau = 0$. Similarly because of the discontinuity at $\tau = t$, instead of a single summation range $k = 1..N$, the summation range has been broken down to two ranges, $k = 1..J$ in (26) and $k = J+1..N$ in (27), where J, $N-J$ are the number of

positive and negative eigenvalues respectively in the eigensolution of (21).

Multiplying both sides of equation 28 by $\alpha_i \Phi^m(\nu_\beta, \mu_i)$ and summing it for $1 \leq i \leq N$ and $1 \leq \beta \leq J$, and using the orthogonality property of the eigenvectors [Barichello et al. 2000]:

$$\sum_{i=1}^{N} \alpha_i \mu_i \Phi_j^m(\mu_i) \Phi_k^m(\mu_i) = 0, \quad j \neq k \tag{29}$$

we find:

$$A_{\beta,\gamma}^m = \frac{\alpha_\gamma \Phi_\beta^m(\mu_\gamma)}{\sigma_\beta^m}, \qquad \sigma_\beta^m = \sum_{i=1}^{N} \alpha_i \mu_i \Phi_\beta^m(\mu_i) \tag{30}$$

In the same manner, multiplying (28) by $\alpha_i \Phi^m(\nu_\beta, \mu_i)$ and summing it for $1 \leq i \leq N$ and $J+1 \leq \beta \leq N$ leads to the following expression:

$$B_{\beta,\gamma}^m = \frac{\alpha_\gamma \Phi^m \beta(\mu_\gamma)}{\sigma_\beta^m} \tag{31}$$

We replace A and B constants in (26,27) and combine the two terms to get a full formulation for our Green's function. We can now compute the particular solution I_p for a given incoming direction μ_{inc} by substituting the resulting Green's function in equation (25):

$$I_p^m(\tau, \mu_i) = \sum_{j=1}^{J} \mathscr{A}_j^m(\tau) \Phi_j^m(\mu_i) + \sum_{j=J+1}^{N} \mathscr{B}_j^m(\tau) \Phi_j^m(\mu_i) \tag{32}$$

where we introduced:

$$\mathscr{A}_j^m(\tau) = \int_0^\tau \sum_{k=1}^{N} A_{j,k}^m(\mu_k) Q^m(t, \mu_k) e^{-(\tau - t)/\nu_j} dt \tag{33}$$

$$\mathscr{B}_j^m(\tau) = -\int_\tau^{\tau_0} \sum_{k=1}^{N} B_{j,k}^m(\mu_k) Q^m(t, \mu_k) e^{(t-\tau)/\nu_j} dt \tag{34}$$

Since Q^m, A^m and B^m are all exponential functions of τ, $\mathscr{A}_j^m$ and $\mathscr{B}_j^m$ have analytical solutions:

$$\mathscr{A}_j^m(\tau) = \mu_0 \nu_j a_j C(\tau, \nu_j, \mu_{inc}) \tag{35}$$

$$\mathscr{B}_j^m(\tau) = \mu_0 \nu_j b_j e^{-\tau/\mu_0} S(\tau_0 - \tau, -\nu_j, \mu_{inc}) \tag{36}$$

with

$$a_j = \frac{1}{\sigma_j^m} \sum_{i=1}^{N} \frac{\alpha_i \omega}{4} \Phi_j^m(\mu_i) p^m(\mu_j, \mu_{inc}) I_{inc}(\mu_{inc}) \tag{37}$$

$$b_j = -\frac{1}{\sigma_j^m} \sum_{i=1}^{N} \frac{\alpha_i \omega}{4} \Phi_j^m(\mu_i) p^m(\mu_j, \mu_{inc}) I_{inc}(\mu_{inc}) \tag{38}$$

and

$$C(\tau, \nu, \mu) = \frac{e^{-\tau/\nu} - e^{-\tau/\mu}}{\nu - \mu}, \quad S(\tau, \nu, \mu) = \frac{1 - e^{-\tau/\nu} e^{-\tau/\mu}}{\nu + \mu} \tag{39}$$

4.3 Computing I^m and BRDF

Having computed the homogeneous solution and the particular solution, we can compose our I^m terms as

$$I^m(\tau, \mu_i) = I_h^m(\tau, \mu_i) + I_p^m(\tau, \mu_i) \tag{40}$$

Note that we still have N unknown L_j^m's in the expression of I_h^m (see equation 23). We finally compute these unknowns by using the boundary conditions at the top and bottom of the plane parallel material layer. BRDF computation (1) assumes that light is incident for only one direction at a time, and this incidence has already been taken into account in the inhomogeneous term. So the radiance field at $\tau = 0$ for all negative angles is zero:

$$I_h^m(0, \mu_i) + I_p^m(0, \mu_i) = 0 \tag{41}$$

where μ_i's are negative.

Similarly, we may assume that material layer is placed on the top of black body base material, and no light is entering from the bottom. So the radiance field at $\tau = \tau_0$ for all positive angles is zero:

$$I_h^m(\tau_0, \mu_i) + I_p^m(\tau_0, \mu_i) = 0 \tag{42}$$

where μ_i's are positive.

Each of these boundary conditions account for $N/2$ equations, so a total of N equations for N unknowns. We solve for the unknown L_i^m's by solving the system of equations.

Note that it is not required to assume a black body interface at the bottom of the layer. If we know the BRDF of the base material on top of which our plane parallel material is placed, then we can compute the radiance field for the positive angles at $\tau = \tau_0$ from the the radiance field for the negative angles at the same location and the BRDF of the base material, and get the required $N/2$ equations. (For all our computation in the next section we have assumed black body base).

We are now ready for computing the BRDF, for which we need the radiance field for all positive angles at the top of the material layer. That means we need $I(0, \mu, \phi)$ for all $\mu > 0$. For this we first formulate a solution for I^m from (16) as:

$$I^m(\tau, \mu) = I^m(\tau_0, \mu) e^{-(\tau_0 - \tau)/\mu} + \frac{1}{\mu} \int_\tau^{\tau_0} (J^m(t, \mu) + Q^m(t, \mu)) e^{-(t-\tau)/\mu} dt \tag{43}$$

where $I^m(\tau_0, \mu)$ is computed using the bottom boundary condition, Q^m follows equation 9 and J^m is substituted by its discrete expression:

$$J^m(\tau, \mu) = \frac{\omega}{2} \sum_{j=1}^{N} \alpha_j p(\mu, \mu_j) I^m(\tau, \mu_j) \tag{44}$$

$I^m(\tau, \mu)$ is known for the quadrature angles μ_i and, as Q^m, is an exponential function of τ. Therefore, the integral in (43) has an closed-form solution. We then compute $I(0, \mu, \phi)$'s for $\phi \in [0..2\pi]$ from $I^m(0, \mu_i)$ using equation 5. Finally we use $I(0, \mu, \phi)$ in equation 1 to compute BRDF for all the user defined μ, ϕ, and μ_{inc} values.

4.4 Multiple layers

At this point we know how to compute the radiance field in a single homogeneous layer. These computations can be extended to a material composed of N_z homogeneous layers placed one on top of the other (Figure 3). The single layer computations discussed earlier in this section can be applied independently to find I^m's at each layer as a combination of both homogeneous and particular solutions for the layer. However, one thing remains to be computed: the N unknown constant L_k^m's for each layer that are used to combine individual eigenvectors based homogeneous solutions (see equation 23). In section 4.3, we discussed how to compute them for a single layer. To extend that method to multiple layers, we need

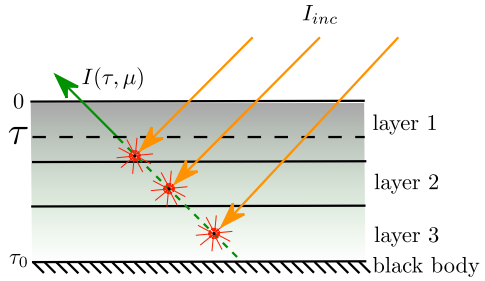

Figure 3: Material composed of three plane-parallel layers. To compute the radiance at a depth τ, the RTE must be solved in each layers.

to compute $N_z \times N$ unknowns and so we need $N_z \times N$ linear equations to solve for these unknowns. The two boundary conditions (41) and (42) of the top surface and bottom surface of the first and the last layer respectively make N linear equations. The remaining $(N_z-1)\times N$ equations come from the (N_z-1) interfaces between N_z layers. Radiance has to be continuous at the interface between the layers. Therefore, using $I_z^m(\tau)$ to denote the radiance field at layer z, and τ_z to denote the optical thickness at the bottom of that same layer we write:

$$I_z(\tau_z,\mu_i) = I_{z+1}(\tau_z,\mu_i), \quad z \in \{1,\cdots,N_z-1\}, i \in \{1,\cdots,N\} \quad (45)$$

Thus in total we get $N_z \times N$ equations. We solve this linear set of equations to compute the unknown L_k^m's for all the N_z layers.

4.5 Algorithm

We summarize all the steps of the solution in algorithm 1.

Algorithm 1 main()

```
1: for m = 0 to L do
2:     ComputeHomogeneous();
3:     ComputeGreensFunction();
4:     for inc = 1 to N do
5:         ComputeParticular(μ_inc);
6:         ComputeRadianceField(μ_inc);
7:     end for
8: end for
9: ComputeReconstructedRadianceField(τ = 0);
10: ComputeBRDF();
```

`ComputeHomogeneous()` solves the eigenproblem defined in section 4.1, giving us all the eigenvectors (Φ^m's) and eigenvalues (ν's). Computations detailed in section 4.2 are carried out in `ComputeGreensFunction()` and in `ComputeParticular()`. `ComputeGreensFunction()` uses the eigensolution to compute the coefficients $A^m_{\beta,\gamma}$ and $B^m_{\beta,\gamma}$ as defined in equations 30 and 31 for equation 32. `ComputeHomogeneous()` and `ComputeGreensFunction()` being independent of the incident light direction, are computed once and are used for every incident direction.

`ComputeParticular()` computes the values of $\mathscr{A}_j^m$ and $\mathscr{B}_j^m$ (equations 35 and 36) for every μ_{inc} of the incident direction, so that the particular solution can be fully reconstructed. `ComputeRadianceField()` computes the constants L_j^m using the method presented in section 4.3.

Once the computations is completed for each order of expansion and each incident direction, `ComputeReconstructedRadianceField()` computes the full radiance field at the surface of the material for any incident and outgoing direction using equation 43, and `ComputeBRDF()` computes the BRDF using equation 1. Note that integrand of equation 43 that depend on the variable t are the exponential terms, so this integration is computed analytically.

5 Results

We implemented the algorithm described in the previous section in C++ language. We used the EIGEN library [http://eigen.tuxfamily.org] for computing eigensolutions and matrix inversions. The input to the solver are: the number of layers composing the material, as well as the coefficients of the phase function, the single scattering albedo and the optical thickness for each of the layers, the number of zenith and azimuth angles for the discrete BRDF table, the number of quadrature nodes and weights. Using this solver we computed the BRDF and stored the result in tabular form. For all of the results shown in this section, we used tables of size $41 \times 41 \times 91$, which corresponds to 41 discrete zenith angles in the range $(0, \frac{\pi}{2})$ for incident and outgoing directions, and 91 relative azimuth angles in the range $[0,\pi]$. For the quadrature, we used 82 Gaussian nodes and weights. The order of the Fourier expansion depended on the phase functions considered, ranging from 15 to 26 for the examples shown in this section. We used 650nm, 533nm, 480nm as representative wavelengths of the RGB color channels and created the BRDF table. Note that for accurate reproduction of material appearance, computation must be carried out at a large number of wavelengths in the visible range.

The materials in our implementation are composed of one or more transparent layers with spherical particles of different sizes embedded inside. Layers are distinguished from each other by the type of particles. We use power law distribution [Hansen and Travis 1974] for the size of the particles in every layer. The coefficients of phase function (g_m's) and single scattering albedos (ω's) for each layer is computed from the refractive index of the particle using Lorenz-Mie theory [van de Hulst 1981]. We use refractive indices of the various materials from SOPRA optical data base [http://www.sspectra.com/sopra.html].

To validate our implementation, we compared our results against those obtained using DISORT [Stamnes et al. 1988], a standard RTE solver. We provide a comparison of the BRDF lobes in figure 4. The shape clearly indicates that using Lambertian model for the diffuse BRDF components will be a gross approximation.

We demonstrate the efficiency of Green's function based particular solution in figure 5, which shows the time needed to compute the particular solutions using our method as a function of the number of incident directions, and compare it with traditional substitution technique. For this comparison we implemented both our Green's function based solution and traditional solution in our solver, generated the timing data keeping the rest of the computations identical. The graph shows that for smaller number ($<$15) of incident directions, our Green's function based method is more expensive compared to the traditional method. This can be explained by the fact that an extra overhead is incurred in the incident direction independent part of the Green's function method i.e. for computing the coefficients $A^m_{\beta,\gamma}$ and $B^m_{\beta,\gamma}$ in equations 30 and 31. This extra overhead is amortized over the computation for multiple incident directions. The amortized cost becomes smaller as the number of incident directions is increased. This is evident from the reduced

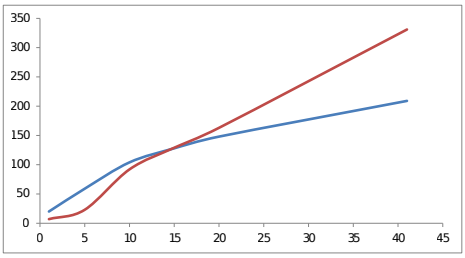

Figure 5: The figure plots the time (in seconds) for computing the particular solution as a function of the number of incident directions. The plot in blue shows the time using Green's function and the plot in red shows the time using the standard method (given in Appendix). The results are computed for a material (composed titanium dioxide particles) with scattering albedo $\omega = 1$, and the order of expansion $L = 26$.

(a) $\tau = 0.1$ (b) $\tau = 1$ (c) $\tau = 5$ (d) $\tau = \infty$

Figure 7: Images rendered using the diffuse BRDF computed for a material layer of different optical thicknesses. The material is composed of spherical hafnium oxide particles embedded in a transparent layer placed on the top of a black body base.

slope of the plot (in blue) for a number of incident directions greater than 15. It is important to note that accurate BRDF computation requires computation of radiance field for large number of incident directions, and our Green's function based method does provide an overall computation efficiency.

Figure 6 shows the Stanford dragon model rendered with diffuse only BRDF computed for a thick material layer composed of different types particles. Figure 7 shows the Stanford Buddha model rendered with diffuse only BRDF computed for a material layer of different thickness. Figure 8 shows conference logo layer painted on the top of a base thick material layer. The base layer is composed of titanium dioxide particles and the logo layer is composed of titanium nitride particles. All of the images were rendered using direct lighting due to a single directional light source.

Figure 8: Image of a thick material layer of titanium dioxide particles with SCCG conference logo painted with a thin layer (0.1 optical thickness) composed of titanium nitride particles.

6 Conclusion

In this paper we presented a Green's function based solution method to the radiative transport equation in a plane parallel medium. We validated our method by comparing BRDF computed by our method with results obtained using a standard RTE solvers. We demonstrated the computed BRDF lobes for several materials, and showed the renderings using these lobes. As a future work, we plan (a) to use a GPU based eigen solver and linear systems solver to speed up our computation, (b) to extend the current method to compute polarized BRDF and (c) to explore the possibility of developing a Green's function only solution that would avoid the computation of radiance field in the whole material volume.

Acknowledgements

This work was supported in part by NSF grant IIS-1064427.

A Computing particular solution

In this appendix, we present the standard method (i.e. without using the Green's function) of computing the particular solution I_p^m to the inhomogeneous equation 16. One common approach to finding such a solution is to express it in the same form as the inhomogeneous source term $Q^m(\tau,\mu_i)$ in that equation. To simplify the discussion we rewrite $Q^m(\tau,\mu_i)$ shown in (9) as:

$$Q^m(\tau,\mu_i) = X^m(\mu_i)e^{-\tau/\mu_{inc}} \tag{46}$$

So the particular solution we seek can be expressed as:

$$I_p^m(\tau,\mu_i) = Z^m(\mu_i)e^{-\tau/\mu_{inc}} \tag{47}$$

Substituting (46) and (47) in (16) and using the relationship

$$\frac{\partial I_p^m(\tau,\mu_i)}{\partial \tau} = -\frac{1}{\mu_{inc}} Z^m(\mu_i)e^{-\tau/\mu_{inc}} \tag{48}$$

we get:

$$(1-\frac{\mu_i}{\mu_{inc}})Z^m(\mu_i) - \sum_{j=1}^{N} \alpha_j p^m(\mu_i,\mu_j)Z^m(\mu_j) = X(\mu_i) \tag{49}$$

So we have a system of N linear equations with N unknown Z^m's. We can use a linear system solver to compute these unknowns. Note that as the coefficients of the linear equations are going to change for every change in incident direction, using this method of particular solution would require us to repeatedly solve a linear system every time. We implemented this approach to generate the comparison results in figure 5.

References

BARICHELLO, L., GARCIA, R., AND SIEWERT, C. 2000. Particular solutions for the discrete-ordinates method. *Journal of Quantitative Spectroscopy and Radiative Transfer 64*, 3, 219 – 226.

CHANDRASEKHAR, S. 1960. *Radiative transfer*. Dover publications.

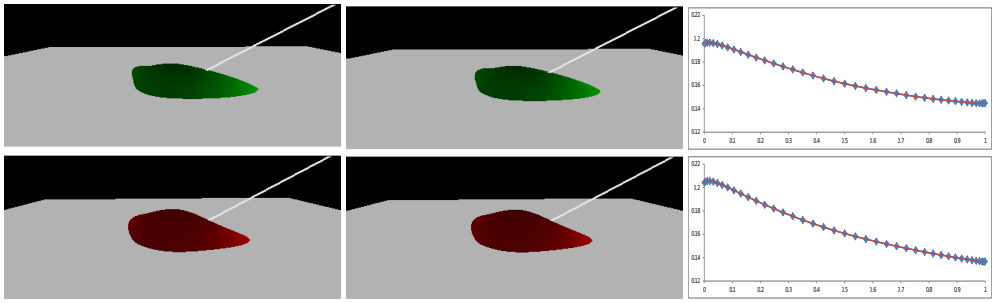

(a) Our method (b) DISORT (c) Comparison

Figure 4: Images in (a), (b) show the lobes computed for a material composed of gallium phosphide particles using our method and is compared with lobes computed using DISORT, a standard RTE solver. Figures in (c) plot the BRDF values (from our method in red and from DISORT in blue) for 41 incident zenith angles keeping azimuth angle fixed. The maximum relative error is 2.10^{-3}. The images on the top row are for the green channel and on the bottom row are for the red channel.

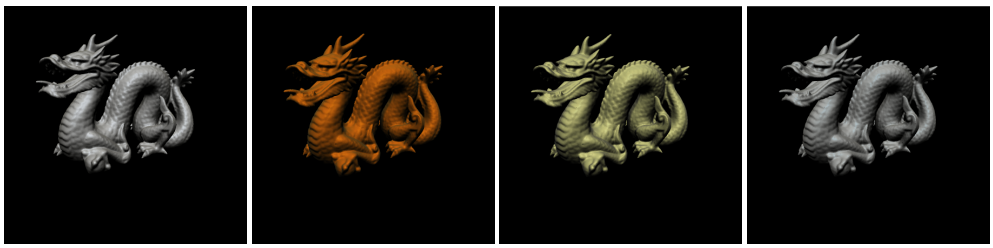

(a) (b) (c) (d)

Figure 6: Images rendered using the diffuse BRDF computed for materials composed of different types of particles: Hafnium Oxide (a), Aluminium Gallium Arsenide (b), Gallium Phosphide (c) and Silicon Oxynitride (d).

DE HAAN, J. F., BOSMA, P. B., AND HOVENIER, J. W. 1987. The adding method for multiple scattering calculations of polarized light. *Astronomy and Astrophysics 183* (Sept.), 371–391.

DORSEY, J., EDELMAN, A., JENSEN, H. W., LEGAKIS, J., AND PEDERSEN, H. K. 1999. Modeling and rendering of weathered stone. In *Proceedings of the 26th annual conference on Computer graphics and interactive techniques*, ACM Press/Addison-Wesley Publishing Co., SIGGRAPH '99, 225–234.

DORSEY, J., RUSHMEIER, H., AND SILLION, F. 2008. *Digital Modeling of Material Appearance*. Morgan Kaufmann Publishers Inc., San Francisco, CA, USA.

HAASE, C. S., AND MEYER, G. W. 1992. Modeling pigmented materials for realistic image synthesis. *ACM Transactions on Graphics (TOG) 11*, 4, 305–335.

HANRAHAN, P., AND KRUEGER, W. 1993. Reflection from layered surfaces due to subsurface scattering. In *Proceedings of the 20th annual conference on Computer graphics and interactive techniques*, ACM, 165–174.

HANSEN, J. E., AND TRAVIS, L. D. 1974. Light scattering in planetary atmospheres. *Space Science Reviews 16* (Oct.), 527–610.

HENYEY, L. G., AND GREENSTEIN, J. L. 1941. Diffuse radiation in the Galaxy. *The Astrophysical Journal 93* (Jan.), 70–83.

JENSEN, H. W., MARSCHNER, S. R., LEVOY, M., AND HANRAHAN, P. 2001. A practical model for subsurface light transport. In *Proceedings of the 28th annual conference on Computer graphics and interactive techniques*, ACM, 511–518.

KUBELKA, P. 1948. New contributions to the optics of intensely light-scattering materials. part i. *JOSA 38*, 5, 448–448.

NICODEMUS, F. E. 1967. Radiometry. In *Vol IV of Applied Optics and Optical Engineering*, New York: Academic.

PHARR, M., AND HANRAHAN, P. 2000. Monte carlo evaluation of non-linear scattering equations for subsurface reflection. In *Proceedings of the 27th annual conference on Computer graphics and interactive techniques*, ACM Press/Addison-Wesley Publishing Co., 75–84.

SOBOLEV, V. V. 1975. *Light Scattering in Planetary Atmospheres*. Pergamon Press.

STAM, J. 1995. Multiple scattering as a diffusion process. In *Rendering Techniques'95*, 41–50.

STAMNES, K., TSAY, S.-C., JAYAWEERA, K., WISCOMBE, W., ET AL. 1988. Numerically stable algorithm for discrete-ordinate-method radiative transfer in multiple scattering and emitting layered media. *Applied Optics 27*, 12, 2502–2509.

VAN DE HULST, H. 1981. *Light scattering by small particles*. Dover publications.